Original Article

Radiomics-based texture and shape analysis to differentiate between lipoma and liposarcoma on magnetic resonance imaging

Chitsanucha Pantawee, M.D.[1, 2]
Jaravee Lasode, M.Sc.[1]
Yothin Rakvongthai, Ph.D.[3, 4]
Jindarat Ratanakornphan, M.D.[2]
Aticha Ariayachaipanich, M.D.[1, 2]
From [1]Division of Diagnostic Imaging, [3]Chulalongkorn University Biomedical Imaging Group, [4]Division of Nuclear Medicine, Department of Radiology, Faculty of Medicine, Chulalongkorn University, Bangkok, Thailand,
[2]Department of Radiology, King Chulalongkorn Memorial Hospital, Bangkok, Thailand.
Address correspondence to A.A (email: Aticha.a@chulahospital.org)

Received 21 September 2025; revised 23 April 2026; accepted 26 April 2026
doi:10.46475/asean-jr.v27i2.987

Abstract

Objective: This retrospective study aimed to assess the utility of magnetic resonance texture and shape analysis (MRTA) in enhancing the diagnostic accuracy of lipoma and liposarcoma differentiation on preoperative magnetic resonance imaging (MRI).

Materials and Methods: A total of 89 cases with pathologically confirmed lipoma or liposarcoma that underwent MRI before surgery at King Chulalongkorn Memorial Hospital between January 2010 and December 2022, were retrospectively included in this IRB-approved study. Axial T1-weighted (T1WI) and axial T1-weighted fat-saturated post-contrast (T1WI FS Gd) images were processed and segmented using the 3D Slicer program. Feature extraction was performed using PyRadiomics. Models were trained and internally validated using 5-fold stratified cross-validation and diagnostic accuracy was compared between MRTA and a musculoskeletal radiologist.

Results: Among 89 lesions (51 lipomas, 38 liposarcomas), MRTA demonstrated a sensitivity and specificity of 74.6% and 94.7%, respectively, on T1WI, and 77.6% and 97.4%, respectively, on T1WI FS Gd. MRTA demonstrated comparable or incrementally improved diagnostic performance compared with radiologist interpretation.

THE ASEAN JOURNAL OF RADIOLOGY
ISSN 2672-9393

Conclusion: MRTA can effectively differentiate lipoma from liposarcoma, with higher sensitivity and specificity than visual radiological assessment. Segmentation on both T1WI and T1WI FS Gd sequences showed that contrast-enhanced fat-suppressed imaging provides superior diagnostic performance by more effectively highlighting enhancing septa and non-lipomatous components.

Keywords: Atypical lipomatous tumor, Lipoma, Liposarcoma, Radiomics, Shape analysis, Texture analysis.

Introduction

Lipomatous soft tissue tumors are the most common mesenchymal neoplasms, ranging from benign to aggressive malignant tumors [1]. Lipoma is a common benign subcutaneous tumor composed of adipose tissue that typically grows slowly. Liposarcoma is among the most prevalent soft tissue sarcomas (STS), accounting for approximately 50% of retroperitoneal and 25% of extremity STS [2]. Liposarcomas are usually managed with surgery and may require adjuvant therapy [3,4] while lipomas often require no treatment unless symptomatic. Accurate diagnosis is therefore essential to guide appropriate treatment and follow-up management.

Magnetic resonance imaging (MRI) is the standard modality for evaluating lipomatous tumors [5]. Several MRI features including tumor size, location, presence of thick septa or enhancement, have been proposed as diagnostic indicators. However, substantial overlap exists between lipomas and liposarcomas [6]. Visual assessment of texture by radiologists remains subjective, leading to a risk of misinterpretation as well as inter- and intra-observer variability [7]. Computer-assisted diagnosis (CAD) has been shown to slightly improve sensitivity, specificity, and accuracy in differentiating liposarcoma from lipoma [8,9].

Radiomic-based texture analysis has emerged as a potential CAD tool for extracting clinically relevant information from tissue heterogeneity within the region of interest (ROI) on conventional imaging, beyond what is perceptible to the human eye. A growing body of research demonstrated that radiomic features can assist in lesion detection, classification, treatment response evaluation, and prognosis prediction in musculoskeletal soft tissue tumors. Magnetic resonance texture analysis (MRTA) has therefore gained attention as a promising adjunct in diagnosing lipomatous tumors. However, existing radiomics studies in lipomatous tumors have several important limitations. These include heterogeneous imaging protocols, variable segmentation strategies (single-slice or two-dimensional analysis versus whole-volume segmentation), incon-

sistent incorporation of contrast-enhanced fat-suppressed sequences, and limited direct comparison with expert musculoskeletal radiologist interpretation. Such methodological variability hinders reproducibility and limits clinical translation. Accordingly, there remains a need for radiomics studies that employ standardized, clinically relevant workflows using routinely acquired MRI sequences.

Therefore, the aim of this study was to develop and internally validate a magnetic resonance texture and shape analysis (MRTA) model using axial T1-weighted imaging (T1WI) and fat-suppressed post-contrast T1-weighted imaging (T1WI FS Gd) to differentiate lipoma from liposarcoma. In addition, we sought to directly compare radiomics-based model performance with that of an experienced musculoskeletal radiologist in a clinically representative setting.

Materials and methods

This retrospective study was approved by the Institutional Review Board (IRB) of our institute, with a waiver of informed consent due to its retrospective design and anonymized data (IRB No. 0540/65). We included patients with pathologically confirmed lipoma or liposarcoma who underwent MRI before surgery at King Chulalongkorn Memorial Hospital between January 2010 and December 2022.

Inclusion criteria were:

- Age >10 years with a lipomatous tumor of the trunk or extremities. Trunk lesions were defined as tumors arising from the chest wall, abdominal wall or back, and did not include mediastinal or retroperitoneal tumors.
- MRI performed prior to surgery with a protocol including axial T1-weighted imaging (T1WI), at least one plane of T2-weighted imaging with fat suppression or short tau inversion recovery (STIR), and axial T1WI with fat suppression and gadolinium contrast (T1WI FS Gd).
- Complete surgical excision of the mass.
- Histopathological confirmation of lipoma or liposarcoma.

Exclusion criteria were:

- Patients who underwent biopsy prior to MRI.
- Recurrent tumors.
- Poor-quality MRI images.
  Based on these criteria, a total of 86 patients with 89 lesions were included. Demographic and clinical data, and histopathological results, were obtained from electronic medical records (EMRs).

THE ASEAN JOURNAL OF RADIOLOGY
ISSN 2672-9393

MRI acquisition
As a tertiary referral hospital, some patients were referred from outside institutions, resulting in variability in MRI scanners and protocols. All examinations were performed using 1.5- or 3.0-Tesla MRI systems.

For most cases, the slice thickness, repetition time (TR), and echo time (TE) were consistent across T1WI and T1WI FS Gd sequences, except for one lesion acquired using a gradient-echo sequence on post-contrast imaging. The median slice thickness was 5.5 mm (range 2.5–8 mm). The median TR was 626 ms (range 420–817 ms for T1WI and 495–817 ms for T1WI FS Gd). The median TE was 12 ms (range 6.0–20.8 ms for T1WI and 6.0–20.8 ms for T1WI FS Gd).

Segmentation
Manual segmentation of all lipomatous tumors was performed using the open-source software 3D Slicer (version 5.5.2; http://download.slicer.org). For each case, regions of interest (ROIs) encompassing the entire tumor volume were delineated on axial T1WI and axial T1WI FS Gd sequences. In all cases, segmentation was performed by a third-year radiology resident and used for feature extraction.

To evaluate interobserver variability, 30 cases (17 lipomas and 13 liposarcomas) were randomly selected and segmented independently by two additional observers (musculoskeletal radiologists with 10 and 11 years of experience, respectively), blinded to pathology and clinical data. Interobserver agreement was assessed using intraclass correlation coefficients (ICCs).

Feature extraction and selection
The segmented ROIs and original MRI images were exported into Python (version 3.9) and processed using the open-source PyRadiomics package (version 3.0.1) [10]. Images were normalized to reduce signal intensity variability. Texture-based, shape-based, and first-order statistical features were extracted from both T1WI and T1WI FS Gd sequences (105 radiomic features per sequence).

To ensure feature stability, intraclass correlation coefficient (ICC) analysis was performed at thresholds of 0.90, 0.95, and 0.99. Subsequently, recursive feature elimination with cross-validation (RFECV) was applied using L2-penalized logistic regression to identify the most informative features. Five-fold stratified cross-validation was performed with the StratifiedKFold function (scikit-learn in Python), maintaining a training-to-validation ratio of 4:1.

Model creation

All selected features from T1WI, T1WI FS Gd and combined sequences (SEs) were used to develop diagnostic models to differentiate lipoma from liposarcoma. We trained multivariate logistic regression classifiers implemented in scikit-learn. Because the proposed approach is a classical machine-learning model using radiomic features, no data augmentation was applied.

Model training and evaluation were performed using 5-fold stratified cross-validation (StratifiedKFold; n_splits = 5, shuffle = True, random_state = 9559), maintaining a training-to-validation ratio of 4:1 in each split. Hyperparameter tuning was performed using GridSearchCV to select the best-performing individual and combined feature sets based on the mean cross-validated AUC. We evaluated L1 (Lasso) and L2 (Ridge) regularization with an inverse regularization strength C in the range 0.0001–100. Optimization was performed using the scikit-learn logistic regression solver (solver = liblinear) with a maximum number of iterations (max_iter = 10000). Training terminated upon solver convergence (default tolerance in scikit-learn) or reaching the maximum iterations (i.e., no separate early-stopping rule was used). Model parameters were initialized using the scikit-learn default setting (no manual initialization). An overview of the radiomics workflow, including segmentation, preprocessing, feature extraction, feature selection, and model training/validation, is summarized in Figure 1.

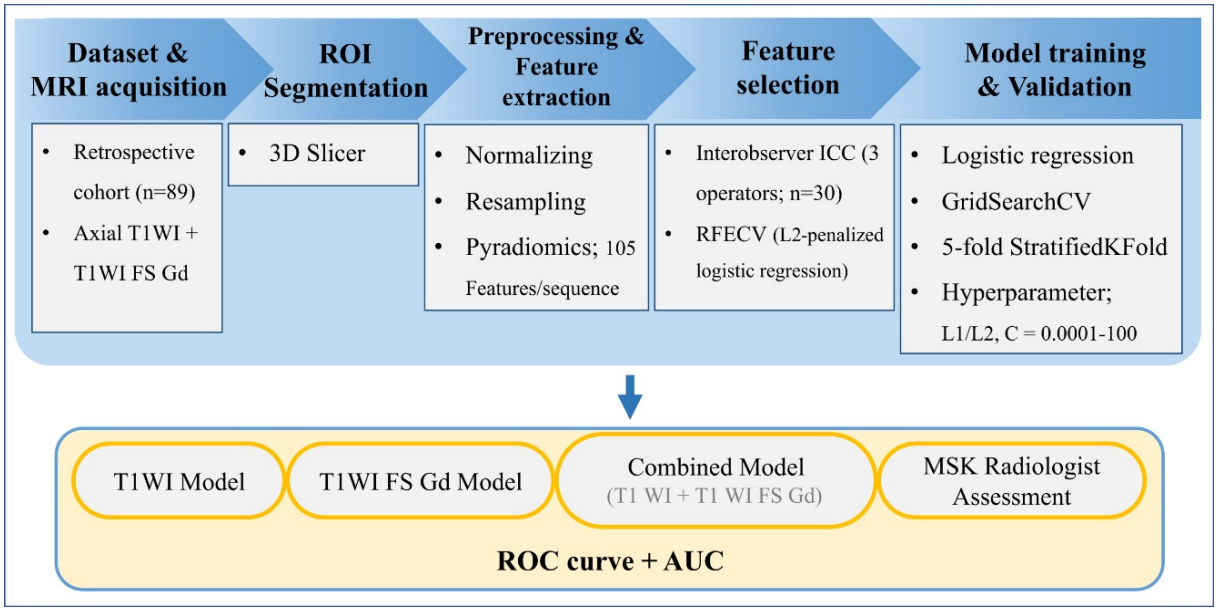

Figure 1. *Study workflow and radiomics pipeline. The flowchart summarizes segmentation, preprocessing, feature extraction, feature selection (interobserver ICC and RFECV), and model training and validation for T1WI, T1WI FS Gd, and combined models, with performance reported as ROC curves and AUC values.*

THE ASEAN JOURNAL OF RADIOLOGY
ISSN 2672-9393

Radiologist diagnosis assessment

An experienced musculoskeletal (MSK) radiologist with 10 years of practice, blinded to clinical and pathological information, independently classified each tumor as either lipoma or liposarcoma. Image interpretation was performed using the Picture Archiving and Communication System (PACS) with Synapse software (Version 5, Fujifilm Global, Japan). For each case, the radiologist reviewed all available MRI sequences, which typically included axial T1WI, at least one plane of T2 FS or STIR, and axial T1WI FS Gd, in accordance with routine clinical practice at our institution. No radiomic features or quantitative outputs were available to the radiologist during interpretation.

Radiological diagnosis was based on established MRI features described in prior studies [11-16]. Lipoma was favored when lesions showed homogeneous fat signal intensity with thin internal septa, complete fat suppression, and no nodular or abnormal enhancement. Atypical lipomatous tumor (ALT) was suspected in predominantly fatty lesions demonstrating atypical features such as a few thickened septa (≥2 mm), focal or septal enhancement, or subtle areas of non-lipomatous components. High-grade liposarcoma was diagnosed when lesions exhibited more aggressive characteristics, including nodular non-lipomatous areas, thick irregular enhancing septa, and heterogeneous internal architecture. For descriptive purposes, radiologists recorded impressions as lipoma, ALT, or high-grade liposarcoma; however, all quantitative analyses were performed using a binary classification of lipoma versus liposarcoma. In addition to classification, the radiologist recorded the tumor depth (superficial, deep, or involving both compartments) and measured the maximum tumor dimension.

Histopathological diagnosis

Histopathological diagnosis, which served as the reference standard, was based primarily on routine morphologic evaluation by experienced musculoskeletal pathologists. Ancillary testing was performed selectively in cases with equivocal histologic features: MDM2 amplification analysis was used to support the diagnosis of atypical lipomatous tumor and was concordant with the final diagnosis in all tested cases, and CDK4 immunohistochemistry was performed in two cases as supportive evidence.

Statistical analysis

All statistical analyses were performed using STATA software (version 18). A two-sided p-value < 0.05 was considered statistically significant. Comparisons of patient demographics and imaging features were conducted using the non-parametric Mann–Whitney test. Interobserver variability of manual segmentation was assessed using intraclass correlation coefficients (ICCs) to evaluate reproducibility between the radiology resident and the two musculoskeletal radiologists.

Diagnostic performance of the computer-assisted models was assessed using the area under the receiver operating characteristic curve (AUC), true positive rate (TPR), and false positive rate (FPR). Sensitivity and specificity were determined using Youden's index derived from the receiver operating characteristics (ROC) analysis of the multivariate logistic regression models. For the radiologist, diagnostic performance was based on a single binary classification per lesion. Sensitivity and specificity were calculated, and the corresponding operating point was plotted in ROC space for comparison with MRTA models. Statistical analyses and performance graphs were generated using Python.

Results

A total of 86 patients with 89 lipomatous lesions were included in the analysis: 51 lipomas and 38 liposarcomas (18 atypical lipomatous tumors [ALTs] and 20 other histologic subtypes of liposarcoma), as shown in Table 1.

Table 1. *Histopathological classification of lipomatous tumors, with atypical lipomatous tumors included in the liposarcoma group. MDM2 amplification testing was performed selectively.*

Lipoma (N=51)	Liposarcoma (N=38)

• Lipoma, not otherwise specified (NOS) (n = 46)*
• Osteochondrolipoma (n = 2)
• Spindle cell lipoma (n = 1) *
• Lipoma with focal myxoid change (n = 2) *
	• Atypical lipomatous tumor (ALT) (n = 18) *
	• High-grade liposarcoma (n = 20)
	  • Dedifferentiated liposarcoma (n = 14)
	  • Myxoid/round cell liposarcoma (n = 4)
	  • Mixed-type liposarcoma (n = 2)

Note * MDM2 amplification testing was performed in selected cases with equivocal histopathologic features; all tested ALT cases (n=12) showed positive MDM2 amplification, whereas all tested lipoma cases (n=15) were negative.	

The mean patient age was 58.7 years (range, 10–83 years). Most lesions occurred in women (52.3%), were located in deep compartments (73%), and most commonly involved the lower extremities (41.6%). The mean maximum diameter of lipomas was 7.6 cm, compared with 14.1 cm for liposarcomas. There were no statistically significant differences between the lipoma and liposarcoma groups with respect to age, sex, tumor depth, or maximum diameter. In contrast, tumor location differed significantly between groups ($p < 0.01$), with liposarcomas occurring more frequently in the lower extremities, whereas lipomas were more commonly located in the upper extremities and trunk. The clinical and demographic characteristics of the study population are summarized in Table 2.

Table 2. *The clinical and demographic characteristics of the patients.*

	All (N=89)	Lipoma (N=51)	Liposarcoma (N=38)	p value
Age (years), mean ± SD	58.7 ± 13.3	56.7	56.6	0.74
Gender				0.40
Male, n (%)	43 (47.7)	25 (49.0)	18 (47.3)	
Female, n (%)	46 (52.3)	26 (51.0)	20 (52.7)	
Anatomical region				<0.001
Upper extremity, n (%)	29 (32.6)	22 (43.1)	7 (18.4)	
Lower extremity, n (%)	37 (41.6)	9 (17.7)	28 (73.6)	
Trunk, n (%)	23 (25.8)	20 (39.2)	3 (8.0)	
Tumor depth				0.28
Superficial, n (%)	20 (22.5)	18 (35.2)	2 (5.3)	
Deep, n (%)	65 (73.0)	30 (58.8)	35 (92.1)	
Both, n (%)	4 (4.5)	3 (6.0)	1 (2.6)	
Longest diameter (centimeters), mean ± SD	10.4 ± 5.5	7.6 ± 3.9	14.1 ± 5.2	0.79

Diagnostic Performance of Radiomics Models

The diagnostic performance of radiomics models was evaluated using multivariate logistic regression analyses across T1WI, T1WI FS Gd, and combined sequences, at different intraclass correlation coefficient (ICC) thresholds (0.90, 0.95, and 0.99). On T1WI, the mean training AUC was 0.91 (SD 0.015), with the mean validation AUCs of 0.89 (SD 0.068). On T1WI FS Gd, the multivariate models achieved the best performance, with a mean training AUCs of 0.94 (SD 0.016) and a mean validation AUCs of 0.94 (SD 0.068). When both sequences were combined, the mean training AUC was 0.964 (SD 0.012) and the mean validation AUC was 0.93 (SD 0.044).

Overall, the T1WI FS Gd multivariate model provided the highest and most consistent diagnostic performance, while the combined model showed comparable performance and the T1WI model achieved slightly lower but still good discrimination.

The three most informative features identified in the multivariate analysis were:
For T1WI: maximum 3D diameter, median first-order intensity, and small dependence high gray-level emphasis.

For T1WI FS Gd: size zone non-uniformity, maximum 3D diameter, and first-order10th percentile intensity.

A comparison of diagnostic performance between the MRTA and an experienced MSK radiologist in multivariate logistic regression model for T1WI, T1WI FS GD and combined. The radiologist provided a single binary interpretation using all available MRI sequences, therefore, the operating point is identical across panels. Visually, the MRTA demonstrated comparable or higher discrimination than the radiologist operating point in ROC space (Figure 2).

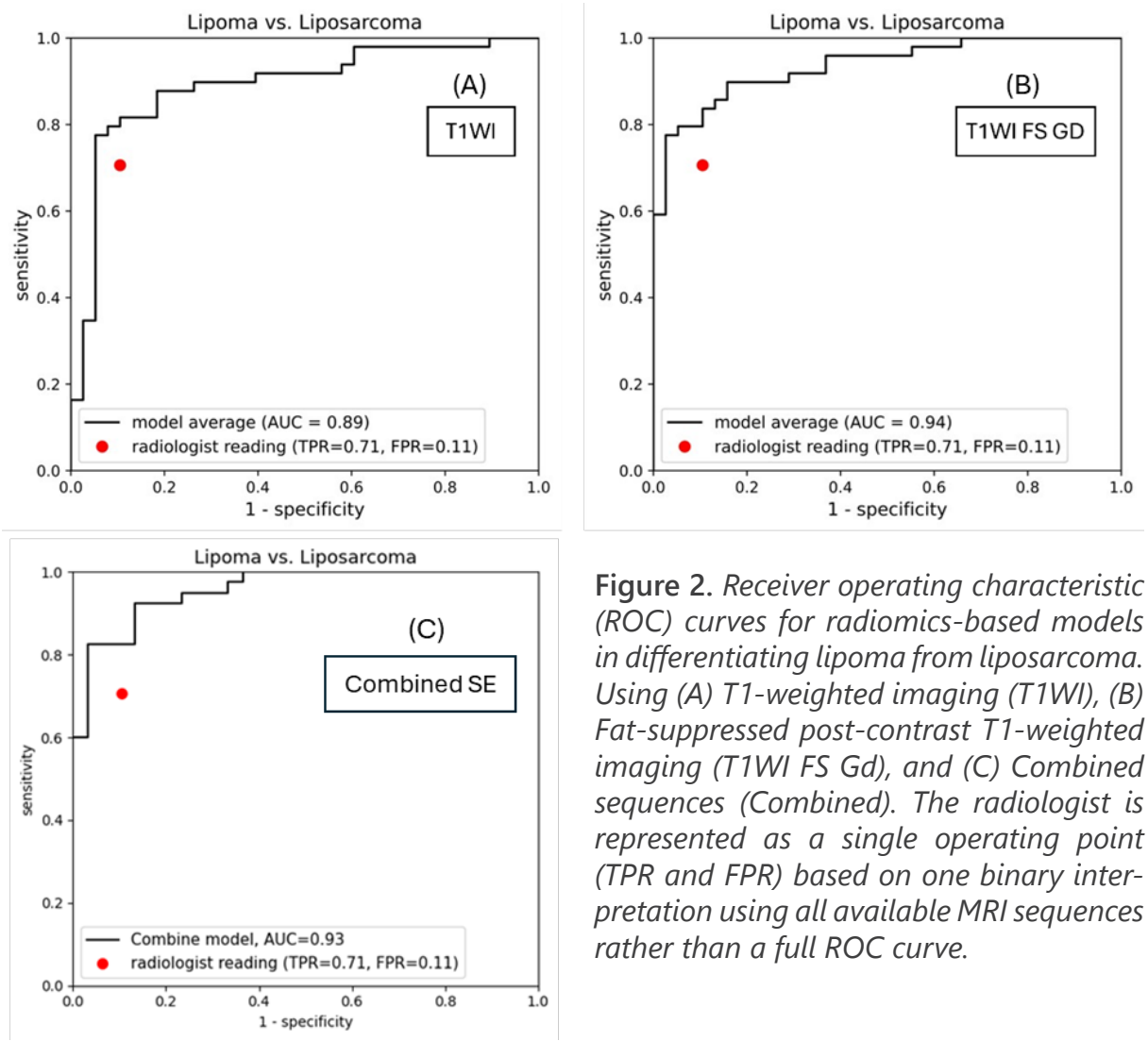

Figure 2. *Receiver operating characteristic (ROC) curves for radiomics-based models in differentiating lipoma from liposarcoma. Using (A) T1-weighted imaging (T1WI), (B) Fat-suppressed post-contrast T1-weighted imaging (T1WI FS Gd), and (C) Combined sequences (Combined). The radiologist is represented as a single operating point (TPR and FPR) based on one binary interpretation using all available MRI sequences rather than a full ROC curve.*

The sensitivity and specificity were calculated using Youden's index derived from receiver operating characteristic (ROC) analysis of the multivariate logistic regression models. On T1WI, MRTA achieved a sensitivity of 74.6% and specificity of 94.7%. On T1WI FS Gd, performance improved further, with a sensitivity of 77.6% and specificity of 97.4%. On combined sequences, MRTA achieved a sensitivity of 85.7% and specificity of 86.8%. The radiologist's operating point lies below the ROC curve of the MRTA model, indicating lower overall discrimination compared with the radiomics-based approach. The radiologist diagnostic performance was a sensitivity of 71% and specificity of 91%

The number of correctly classified and misclassified cases for lipoma, atypical lipomatous tumor (well-differentiated liposarcoma), and other liposarcoma subgroups, as diagnosed by the radiologist, the T1WI multivariate model, and the T1WI FS Gd multivariate model (using Youden's index as the cutoff from ROC analysis), are summarized in Table 3.

Table 3. *Diagnostic performance of radiologist versus MRTA multivariate models in differentiating lipoma, atypical lipomatous tumor, and other liposarcomas. Values represent the number of correctly classified cases (Correct) and misclassified cases (Miss) for each method.*

Diagnosis / Pathology (n)	Radiologist		MRTA on T1WI		MRTA on T1WI FS Gd	
	Correct (n)	Miss (n)	Correct (n)	Miss (n)	Correct (n)	Miss (n)
Lipoma (51)	37	14	41	10	42	9
Atypical lipomatous tumor (18)	14	4	16	2	16	2
Other types of liposarcoma (20)	20	0	20	0	19	1

In the atypical lipomatous tumor and other liposarcoma subgroups, no lesion was misclassified simultaneously by all three methods (radiologist, T1WI multivariate model, and T1WI FS Gd multivariate model).

Notable examples of misclassified cases by the radiologist, MRTA, or both methods are illustrated in Figures 3-6.

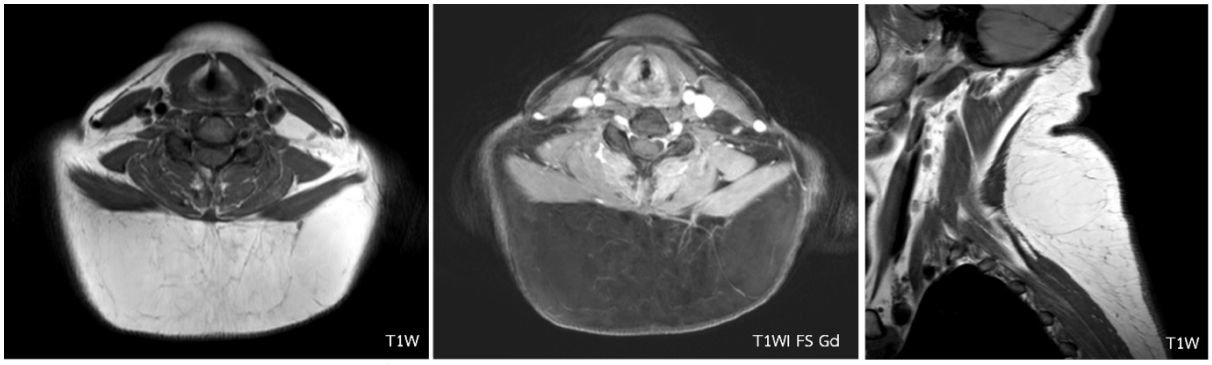

Figure 3. *A neck mass in a 30-year-old woman, diagnosed as subcutaneous lipoma by the radiologist but classified as liposarcoma by both the T1WI and T1WI FS Gd multivariate models. Histopathology confirmed an atypical lipomatous tumor (well-differentiated liposarcoma).*

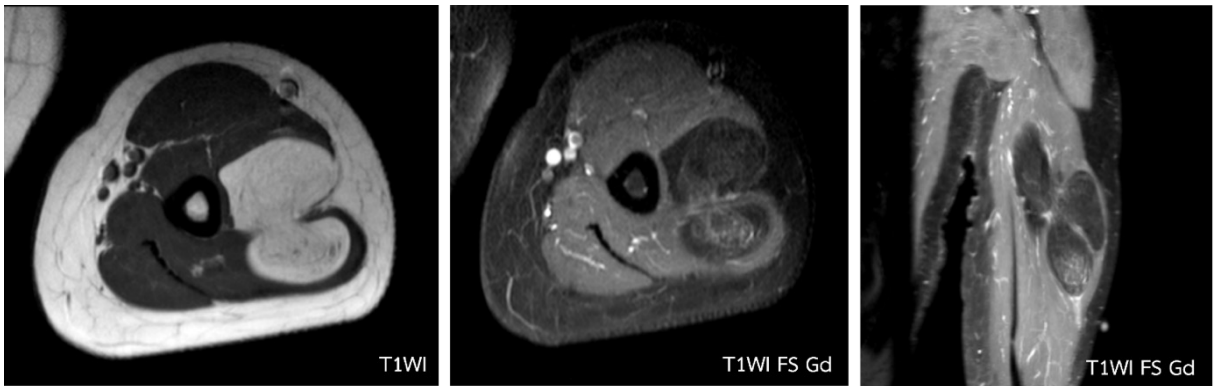

Figure 4. *An arm mass in a 46-year-old woman, diagnosed as liposarcoma by the radiologist and T1WI model, classified as lipoma by the T1WI FS Gd model. Histopathology confirmed an atypical lipomatous tumor.*

Figure 5. *A shoulder mass in a 50-year-old woman, diagnosed as lipoma with intralesional muscle fibers (arrow) by the radiologist and T1WI FS Gd model, classified as liposarcoma by the T1WI model. Histopathology confirmed a lipoma.*

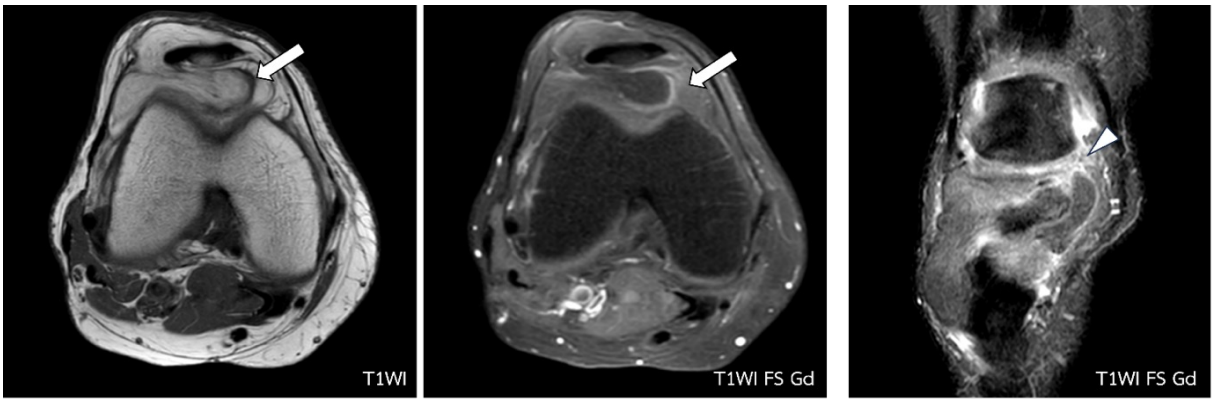

Figure 6. *An anterior knee mass in a 59-year-old woman with thick enhanced internal septation (arrow) and an area of patchy enhancement (arrowhead). The radiologist, T1WI, and T1WI FS Gd models all diagnosed liposarcoma; however, histopathology confirmed a lipoma.*

Discussion

Differentiating lipoma from liposarcoma remains a common and clinically important challenge in musculoskeletal imaging. Conventional MRI features—such as lesion size, internal septation, and enhancement patterns—are helpful but often overlap between benign lipomas and malignant liposarcomas, particularly atypical lipomatous tumors [12-16]. In recent years, radiomics-based approaches have shown promise in improving diagnostic accuracy; however, prior studies have been limited by heterogeneous imaging protocols, two-dimensional or single-slice segmentation, lack of comparison with expert radiologists, and inconsistent use of contrast-enhanced imaging [8-10,17-19]. The strength of the present study lies in its clinically oriented design, combining whole-volume radiomics analysis of routine MRI sequences with direct comparison to an experienced musculoskeletal radiologist. By evaluating both non-contrast T1-weighted and fat-suppressed contrast-enhanced sequences within a standardized workflow, this study addresses key knowledge gaps highlighted in recent reviews and provides new insight into the incremental value of radiomics in routine clinical practice.

According to our results, the radiologist achieved a sensitivity of 71% and specificity of 91%. In comparison, MRTA demonstrated higher performance, with sensitivity and specificity of 74.6% and 94.7% on T1WI, 77.6% and 97.4% on T1WI FS Gd, and 85.7% and 86.8% in the combined model, respectively. These findings suggest that radiomics-based texture and shape analysis may enhance diagnostic efficacy and reduce the risk of misinterpretation. Importantly, in the atypical lipomatous tumor and other liposarcoma subgroups, no lesion was misclassified simultaneously by all three methods (radiologist, T1WI multivariate model, and T1WI FS Gd multivariate model), underscoring the complementary value of MRTA in clinical decision-making.

Beyond overall performance, the selected radiomic features may provide insight into imaging characteristics that may discriminate between benign and malignant lipomatous tumors. For T1WI model, the most informative features (maximum 3D diameter, first-order median intensity, and small dependence high gray-level emphasis) reflect lesion size, signal distribution, and fine-scale texture. For T1WI FS Gd, key features (size zone non-uniformity, maximum 3D diameter, and first-order 10th percentile intensity) highlight post-contrast heterogeneity, which may reflect a more complex internal structure, such as enhancing septa and non-fatty components. Size related features were consistently incorporated into the models, indicating that tumor size contributes meaningfully to malignancy prediction in lipomatous tumors, in line with conventional imaging-based literature [20-22]. In addition, texture features — specifically GLDM- and GLSZM-derived non-uniformity metrics and First-order intensity descriptors were

also retained, suggesting that the pattern of enhancement heterogeneity and internal complexity, rather than enhancement intensity alone, is important for distinguishing benign from malignant lipomatous tumors [18,23]. Together, these findings suggest that radiomics quantitatively captures subtle heterogeneity and internal complexity that may be underappreciated by visual assessment, providing biological plausibility for the observed diagnostic benefit.

Our findings are consistent with and extend prior radiomics studies of lipomatous tumor. Earlier work demonstrated that MRI-based texture and shape analysis and demonstrated improved differentiation between lipoma and liposarcoma [9] and subsequent studies reported high diagnostic accuracy using radiomics derived from contrast T1WI [18,19]. Most recently, Haidey et al. (2023) have systematically reviewed and highlighted the overall promise of radiomics while emphasizing substantial methodological heterogeneity and limited clinical validation [17]. In contrast to many prior studies, the present work applies whole-volume segmentation, evaluates routinely acquired MRI sequences, and directly benchmarks radiomics performance against expert musculoskeletal radiologist interpretation. While large multicenter deep-learning approaches have demonstrated scalability and external validation [21], our manual whole-volume approach provides complementary insight into the specific contribution of contrast-enhanced fat-suppressed imaging and interpretable radiomic features in everyday clinical practice.

Taken together, our findings reinforce the potential of MRTA to improve diagnostic accuracy for lipomatous tumors, especially when applied to contrast-enhanced FS sequences. However, the variability in ROI methodology across studies underscores the need for standardized segmentation protocols. Larger multicenter studies, ideally incorporating automated segmentation approaches similar to those reported by Spaanderman et al. [24], will be essential to validate and generalize these results.

Conclusion

This study demonstrated that magnetic resonance texture and shape analysis (MRTA) can effectively differentiate lipoma from liposarcoma, with higher sensitivity and specificity than visual radiological assessment. Segmentation on both T1WI and T1WI FS Gd sequences showed that contrast-enhanced fat-suppressed imaging provides superior diagnostic performance by better highlighting enhancing septa and non-lipomatous components.

Our findings support MRTA as a promising adjunct to radiologist interpretation, helping to reduce diagnostic uncertainty and misclassification, particularly in challenging cases. Future multicenter studies with larger cohorts, standardized segmentation protocols, and external validation—ideally incorporating automated or semi-automated workflows—will be essential to further validate and generalize these findings.

Conflict of interest

None declared.

References

1. Johnson CN, Ha AS, Chen E, Davidson D. Lipomatous soft-tissue tumors. J Am Acad Orthop Surg 2018;26:779–88. doi: 10.5435/JAAOS-D-17-00045.

2. Crago AM, Dickson MA. Liposarcoma: Multimodality management and future targeted therapies. Surg Oncol Clin N Am 2016;25:761–73. doi: 10.1016/j.soc.2016.05.007.

3. Gronchi A, Miah AB, Dei Tos AP, Abecassis N, Bajpai J, Bauer S, et al. Soft tissue and visceral sarcomas: ESMO-EURACAN-GENTURIS clinical practice guidelines for diagnosis, treatment and follow-up. Ann Oncol 2021;32:1348–65. doi: 10.1016/j.annonc.2021.07.006.

4. Mullen JT, Kobayashi W, Wang JJ, Harmon DC, Choy E, Hornicek FJ, et al. Long-term follow-up of patients treated with neoadjuvant chemotherapy and radiotherapy for large, extremity soft tissue sarcomas. Cancer 2012;118:3758–65. doi: 10.1002/cncr.26696.

5. Sommerville SM, Patton JT, Luscombe JC, Mangham DC, Grimer RJ. Clinical outcomes of deep atypical lipomas (well-differentiated lipoma-like liposarcomas) of the extremities. ANZ J Surg 2005;75:803–6. doi: 10.1111/j.1445-2197.2005.03519.x.

6. Billing V, Mertens F, Domanski HA, Rydholm A. Deep-seated ordinary and atypical lipomas: histopathology, cytogenetics, clinical features, and outcome in 215 tumours of the extremity and trunk wall. J Bone Joint Surg Br 2008;90:929–33. doi: 10.1302/0301-620X.90B7.20348.

7. O'Donnell PW, Griffin AM, Eward WC, Sternheim A, White LM, Wunder JS, et al. Can experienced observers differentiate between lipoma and well-differentiated liposarcoma using only MRI? Sarcoma 2013;2013:982784. doi: 10.1155/2013/982784.

8. Juntu J, Sijbers J, De Backer S, Rajan J, Van Dyck D. Machine learning study of several classifiers trained with texture analysis features to differentiate benign from malignant soft-tissue tumors in T1-MRI images. J Magn Reson Imaging 2010;31:680–9. doi: 10.1002/jmri.22095.

9. Thornhill RE, Golfam M, Sheikh A, Cron GO, White EA, Werier J, et al. Differentiation of lipoma from liposarcoma on MRI using texture and shape analysis. Acad Radiol 2014;21:1185–94. doi: 10.1002/jmri.22095.

10. van Griethuysen JJM, Fedorov A, Parmar C, Hosny A, Aucoin N, Narayan V, et al. Computational Radiomics System to Decode the Radiographic Phenotype. Cancer Res 2017;77:e104–7. doi: 10.1158/0008-5472.CAN-17-0339.

11. Chernev I, Petit-Clair N. Magnetic resonance imaging characteristics of intramuscular lipomas. Sao Paulo Med J 2015;133:64–6. doi: 10.1590/1516-3180.2014.86200716.

12. Doyle AJ, Pang AK, Miller MV, French JG. Magnetic resonance imaging of lipoma and atypical lipomatous tumour/well-differentiated liposarcoma: observer performance using T1-weighted and fluid-sensitive MRI. J Med Imaging Radiat Oncol 2008;52:44–8. doi: 10.1111/j.1440-1673.2007.01910.x.

13. Gupta P, Potti TA, Wuertzer SD, Lenchik L, Pacholke DA. Spectrum of fat-containing soft-tissue masses at MR imaging: The common, the uncommon, the characteristic, and the sometimes confusing. Radiographics 2016;36:753–66. doi: 10.1148/rg.2016150133.

14. Knebel C, Neumann J, Schwaiger BJ, Karampinos DC, Pfeiffer D, Specht K, et al. Differentiating atypical lipomatous tumors from lipomas with magnetic resonance imaging: A comparison with MDM2 gene amplification status. BMC Cancer 2019;19:309. doi: 10.1186/s12885-019-5524-5.

15. Kransdorf MJ, Bancroft LW, Peterson JJ, Murphey MD, Foster WC, Temple HT. Imaging of fatty tumors: distinction of lipoma and well-differentiated liposarcoma. Radiology 2002;224:99–104. doi: 10.1148/radiol.2241011113.

16. Muhib M, Abidi SLF, Ahmed U, Afzal A, Farooqui A, Khalid Jamil OB, et al. Use of radiologic imaging to differentiate lipoma from atypical lipomatous tumor/well-differentiated liposarcoma: Systematic review. SAGE Open Med 2024;12:20503121241293496. doi: 10.1177/20503121241293496.

17. Haidey J, Low G, Wilson MP. Radiomics-based approaches outperform visual analysis for differentiating lipoma from atypical lipomatous tumors: a review. Skeletal Radiol 2023;52(:1089–100. doi: 10.1007/s00256-022-04232-0.

18. Leporq B, Bouhamama A, Pilleul F, Lame F, Bihane C, Sdika M, et al. MRI-based radiomics to predict lipomatous soft tissue tumors malignancy: a pilot study. Cancer Imaging 2020;20:78. doi: 10.1186/s40644-020-00354-7.

19. Pressney I, Khoo M, Endozo R, Ganeshan B, O'Donnell P. Pilot study to differentiate lipoma from atypical lipomatous tumour/well-differentiated liposarcoma using MR radiomics-based texture analysis. Skeletal Radiol 2020;49:1719–29. doi: 10.1007/s00256-020-03454-4.

20. Coran A, Ortolan P, Attar S, Alberioli E, Perissinotto E, Tosi AL, et al. Magnetic resonance imaging assessment of lipomatous soft-tissue tumors. In Vivo 2017; 31:387–95. doi: 10.21873/invivo.11071.

21. Datir A, James SL, Ali K, Lee J, Ahmad M, Saifuddin A. MRI of soft-tissue masses: The relationship between lesion size, depth, and diagnosis. Clin Radiol 2008;63:373–8; discussion 379–80. doi: 10.1016/j.crad.2007.08.016.

22. El Ouni F, Jemni H, Trabelsi A, Ben Maitig M, Arifa N, Ben Rhouma K, et al. Liposarcoma of the extremities: MR imaging features and their correlation with pathologic data. Orthop Traumatol Surg Res 2010;96:876–83. doi: 10.1016/j.otsr.2010.05.010.

23. Wang S, Chan LW, Tang X, Su C, Zhang C, Sun K, et al. A weighted scoring system to differentiate malignant liposarcomas from benign lipomas. J Orthop Surg (Hong Kong) 2016;24:216–21. doi: 10.1177/1602400219.

24. Spaanderman DJ, Hakkesteegt SN, Hanff DF, Schut ARW, Schiphouwer LM, Vos M, et al. Multi-center external validation of an automated method segmenting and differentiating atypical lipomatous tumors from lipomas using radiomics and deep-learning on MRI. EClinicalMedicine 2024;76:102802. doi: 10.1016/j.eclinm.2024.102802.